Available on CMS information server

**CMS NOTE 1997/084**

**The Compact Muon Solenoid Experiment**

# CMS Note

Mailing address: CMS CERN, CH-1211 GENEVA 23, Switzerland

**29 August 1997**

# Muon Track Reconstruction Efficiency of ME1/1 Dubna Prototype in the Integrated Test

I.Golutvin, I.Gramenitsky, P.Moissenz, S.Movchan, V.Palichik, A.Zarubin

*Joint Institute for Nuclear Research, Dubna, Russia*

**Abstract**

The aim of this note is to study a track reconstruction efficiency of muons detected with six-layer CSC and its distortion by electromagnetic secondaries induced by the high energy muon passed through a hadron calorimeter. Experimental data taken in the Integrated Test of CMS endcap detector prototypes were used for analysis.

# 1 Introduction

To achieve of required momentum resolution [1] the CMS muon system should provide a high efficiency of muon track reconstruction with a good spatial resolution. The muon detector is located behind the hadron calorimeter. High energy muons themselves produce a significant number of electromagnetic (e.m.) secondaries passing through the calorimeter matter. A part of e.m. secondaries reaches the muon detector and makes the muon track reconstruction more difficult.

The aim of this note is to estimate a number of electromagnetic secondaries using the experimental data from the muon detector (the P2 prototype of ME1/1) and to study efficiency of muon track reconstruction (by separating muon tracks from secondaries).

# 2 Experimental Setup

The Integrated Test experiment was carried out to test CMS endcap prototypes.

The Integrated Test setup located at the H2 beam line of the CERN SPS accelerator is shown in Fig.1. The prototypes of CMS endcap preshower, electromagnetic calorimeter (ECAL), hadron calorimeter (HCAL) and muon detector (ME1/1) were placed into the superconducting magnet M1. The axial magnetic field was oriented along the beam. The variation of the magnetic field in the ME1/1 was in the range of 2.5-3 Tesla for different layers. Data taking were performed with a negative muon beam of energy 100, 150, 225 and 300 GeV. Iron return yoke of the magnet M2 (switched off) used as an absorber (3.8 m Fe). Muons were identified with S7 scintillator located behind the M2. Track parameters of the incoming muon beam were measured with U1 and U2 beam chambers located in front of the Integrated Test setup.

A full-scale P2 prototype of Cathode Strip Chamber of 1/36 ME1/1 sector is used as a muon detector. Cathode Strip Chamber (CSC) is a six-layer multiwire proportional chamber with cathode strip read-out. Precise position of a charged particle is measured by the ratio of charges induced on several adjacent cathode strips. Spatial resolution of this prototype with $\sim$5 mm strip width was about 50-60 $\mu$m per layer [2].

# 3 Muon Track Reconstruction

A lot of hits in CSC are produced by e.m. secondaries ($\gamma$ and $e^-/e^+$) in addition to muon hits. Muon generated these e.m. secondaries due to $\delta$-rays (also called "$\delta$-electrons"), bremsstrahlung and direct $e^+e^-$-pair production. Bremsstrahlung and pair production cross-section, in energy range of primary muon of several hundreds GeV increase rapidly with energy and produce an e.m. showers which can be close to the muon track and that is why the original muon position may be distorted.

Muon events are selected according to the following criteria:

- negligible energy deposition in the HCAL;
- hit in the S7 scintillator;
- anode hits within a wide (110 mm) road in four (or more) layers out of six (anode wires are arranged to groups of 22 wires each);
- four (or more) cathode layers out of six with clusters within the beam profile.

There are only a few percents of events which do not meet these requirements.

A charge induced by one particle on the cathode layer was distributed onto 3-5 strips. When the charged secondaries pass through the CSC layer at a distance less than 5 strips from the muon position, the induced cathode charges are overlapped and produced a wide clusters (more than 5 strips). A procedure of splitting wide clusters into sub-clusters to correctly define the muon position is developed.

More than 10 % of the cluster information contains an overflow in a strip with the maximum signal because of using 10 bits ADC. Shape parametrisation of the induced cathode charges on the cathode allows to reconstruct the value of overflowed charge. This procedure improve identification of the muon position.

The "ratio" method [3,4] is used for calculation of the x-coordinate of the cathode charge distribution centroid. Muon track candidates are chosen from the $x_i$-array at four (or more) cathode layers out of six in a narrow road (1 mm) according to the algorithm shown in Fig.2.

A muon track is supposed to satisfy the following requirements:

- at least four $x_i$-coordinates must be within the road of 1 mm width and it's slope $|\alpha| < 30 mrad$;
- a track candidate should be inside the beam profile of $\pm 20 mm$.

After line fitting ($x^{fit} = az + b$) with the method of least squares, tracks are classified in three groups.

(i) A "good" $\mu$-track (1st class) must satisfy the goodness-of-fit criterion:

$$R = \sqrt{\sum_{i=1}^{n} (x_i - x_i^{fit})^2 / (n-2)} < 0.35 mm, \qquad (1)$$

where $n$ ($4 \leq n \leq 6$) is the number of points on track. Examples of such events are presented in Figs.3-4. If a track candidate with more than 4 points does not satisfy this criterion, the most distant point from the fitted line is rejected and then the track is re-fitted.

(ii) If the 4-point track candidate does not satisfy the criterion (1), we restore the initial track candidate including all the rejected points. We classify these tracks to be of the 2nd class, calling them " $\mu$-tracks with e.m. secondaries".

If at the beginning of the track search we can not reveal a track candidate in a narrow road, we try to reconstruct a track in a road of 6 mm width with angles $|\alpha| < 60 mrad$. If such a track contains four (or more) points out of six, we classify it as a $\mu$-track with secondaries. This is the case when secondaries distort muon measurements in several planes. An example of such event is presented in Fig.5.

The quality of the reconstructed tracks can be illustrated by residuals ($x_i - x_i^{fit}$). In Fig.7a we present a distribution of residuals for "good" $\mu$-tracks (1st class), cumulated for all chamber planes. The value of mean-root-square error (RMS) is equal to 75 $\mu$m. The "tails" seen in this histogram are caused by $\delta$-rays and secondaries passing too close to muons. Fig.7b shows residuals for the events of the 2nd class with the value of RMS is about 1 mm.

The efficiency of the 1st and 2nd class muon track reconstruction versus the energy of the muon beam is shown in Fig.8. One can see that the number of "good" $\mu$-tracks reduces from 94 % to 91 % and the number of $\mu$-tracks with secondaries grows from 5 % to 8 % when the beam energy increases from 100 GeV to 300 GeV.

(iii) Less than 1 % of the events contain very "hard" e.m. showers and that is why it is impossible to reconstruct any $\mu$-track even in the wide road (events of the 3rd class; see example in Fig.6).

Thus, we have estimated the efficiency of the $\mu$-track reconstruction for the 6-layer CSC. However, some layers may be missing due to technical reasons or strips on some layers are tilted (so named "stereo strips").

From Fig.9 it is clear that if one layer is missed, the efficiency of a $\mu$-track reconstruction decreases by 5 %. The reconstruction of the $\mu$-track with two missing layers decrease an efficiency up to 80 %.

# 4 Electromagnetic Secondaries in the Muon Detector

Most of $\delta$-rays produced inside the chamber have low energy and disappear near the muon track. We classify an event as one with secondaries if an additional cluster ("standing alone") is detected in some CSC layer (i.e. the distance between this charged particle and muon is more than 2 cm).

Since the probability of a $\delta$-electron to be produced in one layer is about 12%, and the probability to reach the next layer is $\sim$20 % [5], then the probability of muon coordinates to be distorted in three planes by $\delta$-electrons is only 5%, which corresponds to the difference between two dotted lines for ME1/1 alone in Fig.10. Thereby we additionally account the events with at least three distorted muon coordinates. From the track reconstruction algorithm one can see that the problem of track reconstruction appears just in this very case. We can estimate the part of the events with e.m. secondaries from calorimeters by summing the events with at least three distorted muon coordinates to the ones with standing along clusters. While increasing the muon beam energy $E_\mu$ from 100 to 300 GeV, the number of these events increases from 20 % to 25 % (see Fig.10). GEANT simulation results of secondaries caused by the muon passing through the Integrated Test setup are in a good agreement with experimental data shown in Fig.10.

Using standing alone clusters and sub-clusters obtained after the wide cluster splitting, we can additionally try to find tracks of accompanying electrons. These tracks are required to have at least three points per track. Fig.11

shows the fraction of events with additional tracks to grow from 6 % to 10 % when the beam energy increasing from 100 to 300 GeV. A significant part of these tracks has only 3 points and does not concurrent with muon tracks.

# 5 Summary

An influence of electromagnetic secondaries production in P2 ME1/1 Cathode Strip Chamber prototype standing alone and one located behind the calorimeters on the muon track reconstruction was studied based on experimental data taken in the Integrated Test of CMS endcap prototypes.

(i) A fraction of high energy muon tracks in CSC stand alone with fatal distortion of clusters in to the three or more layers due to $\delta$-electron production estimated as 5% (see Fig.10). This value is in agreement with our previous measurement with cosmic rays [5].

(ii) The Integrated Test experimental data have shown that the high energy muons (100 - 300 GeV) produces up to 20-25 % of events with electromagnetic secondaries coming to the CSC from the calorimeters.

(iii) Though the muon coordinates were distorted by secondaries, we have managed to obtain an efficiency ($\geq$ 92%) (see Fig.8) of the muon track reconstruction with a rather satisfactory accuracy (as shown in Fig.7) due to splitting of wide clusters into sub-clusters and restoring the charge on strips with overflow.

(iv) The probability of false track generated by e.m. secondaries are variated from 3% for tracks with 3 hits per track to 10% with at least 3 hits per track as shown in Fig.11.

(v) Variation of efficiency of track reconstruction measured by 4 (or more) out of 6,5 or 4 CSC layers from 92% to 80% (see Fig.9), in addition to point (iv), is head out a conclusion that six-layers CSC provide an efficient and precise muon track detection in the energy range of 100-300 GeV.

# 6 References


1. CMS collaboration. The Compact Muon Solenoid, Technical Proposal, CERN/LHCC 94-38, LHCC/P1, 1994.

2. A.Chvyrov, I.Golutvin et al. Bunch crossing identification study on MF1 prototype beam test data. CMS TN/95-161, 1995.

3. J.Chiba et al. Study of position resolution for cathode readout MWPC with measurement of induced charge distribution. NIM, 206 (1983), p.451.

4. A.Chvyrov et al. The spatial resolution of 3x0.3$m^2$ Dubna prototype CSC. SSCL GEM TN-93-466, 1993.

5. C.Albajar et al. Study of electromagnetic secondaries in RD5. NIM, A364 (1995) p.473

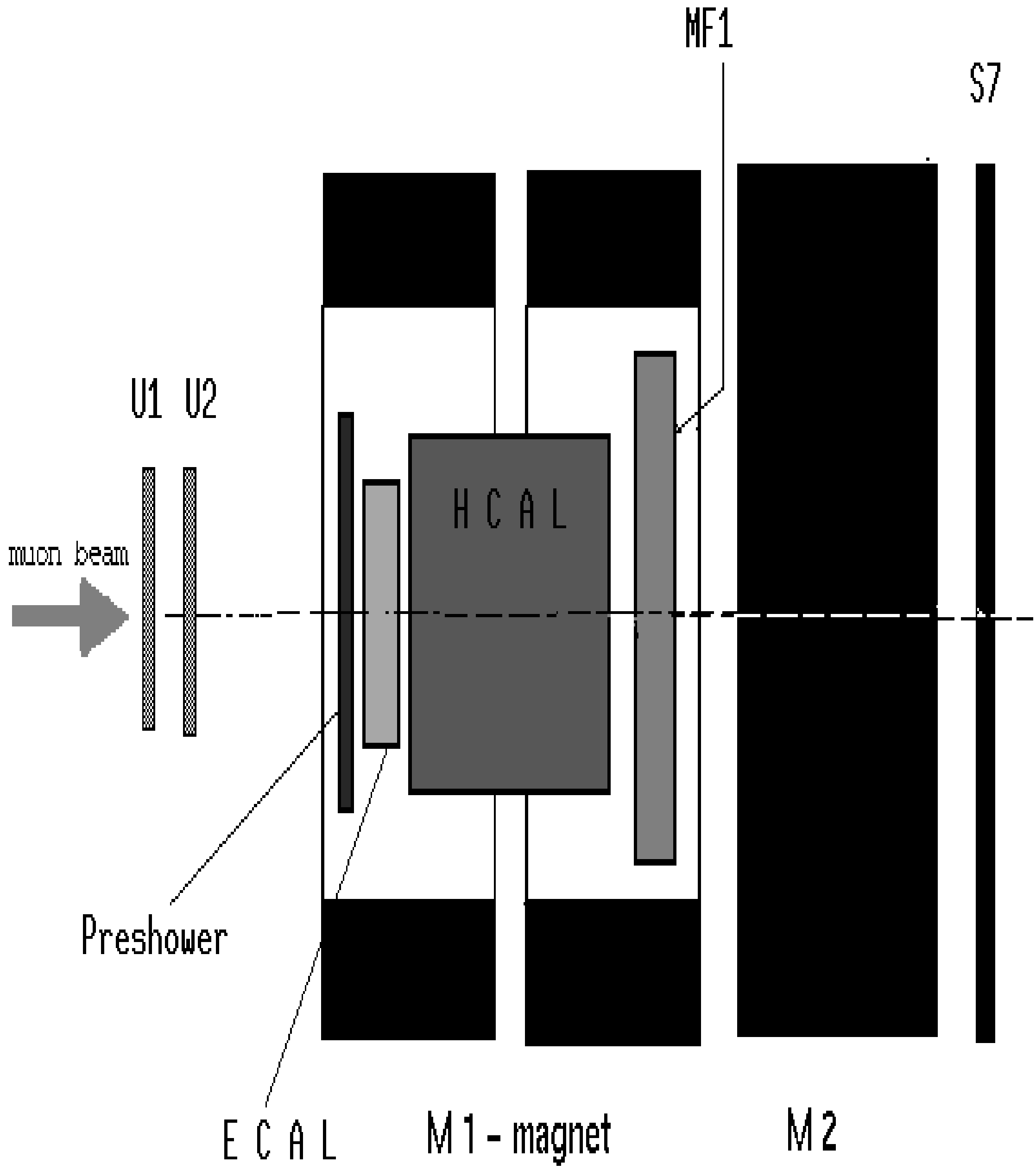


Figure 1: The Integrated Test experimental setup.

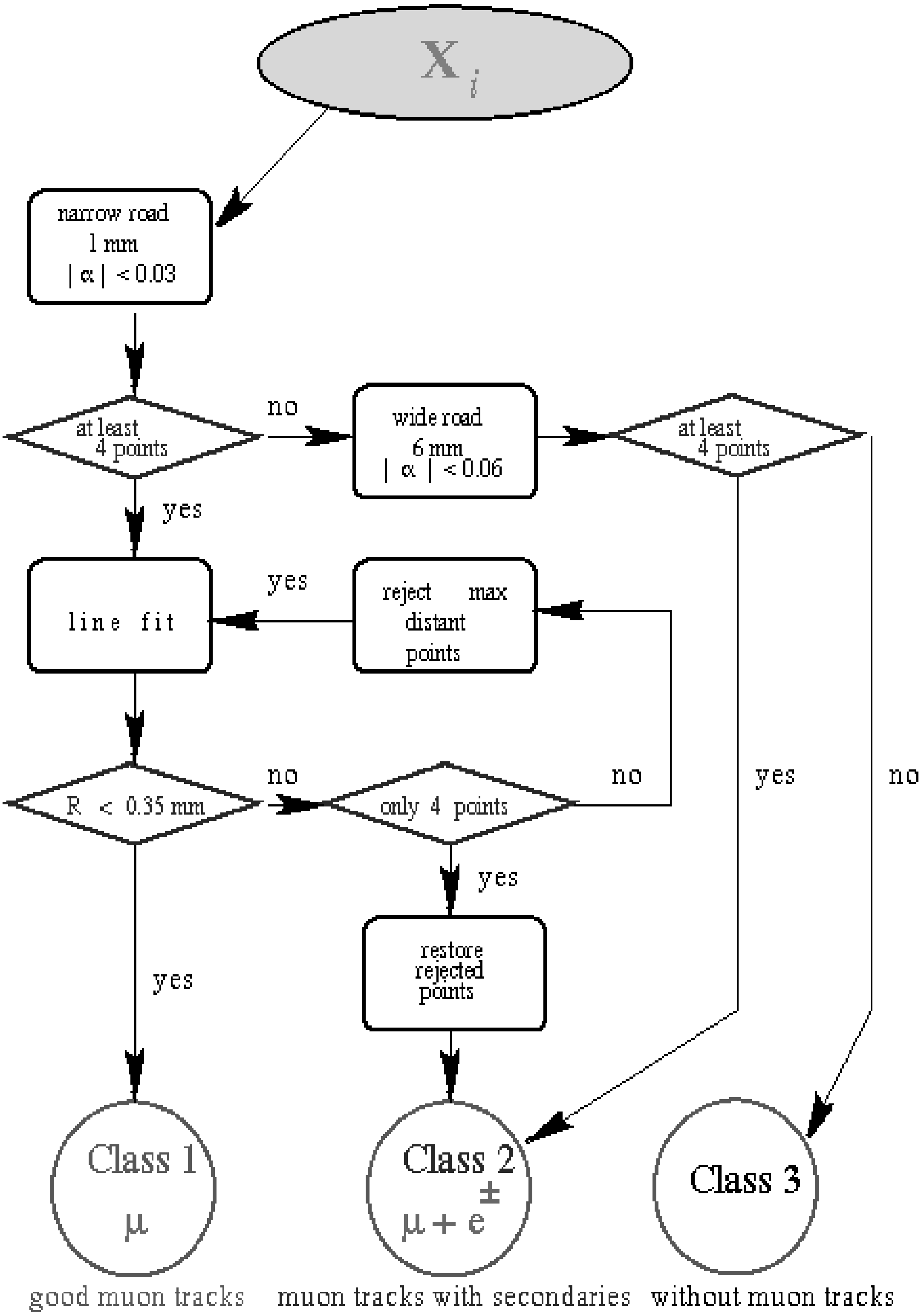


Figure 2: The block-scheme of the muon track reconstruction algorithm.

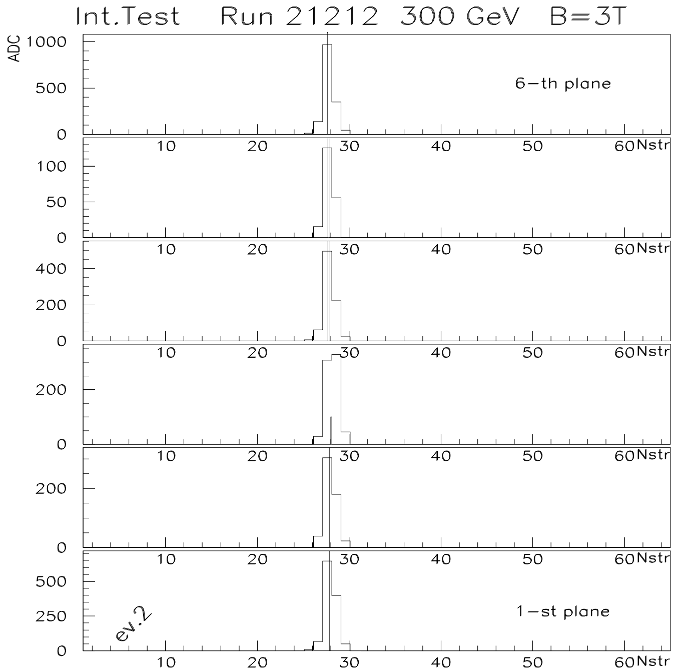


Figure 3: The example of "good" $\mu$-track event. The charge is induced on strips of the six cathode planes of the ME1/1 chamber. The track coordinates are drawn with long segments. The coordinate beyond the track is given with a short segment (on the 3rd plane).

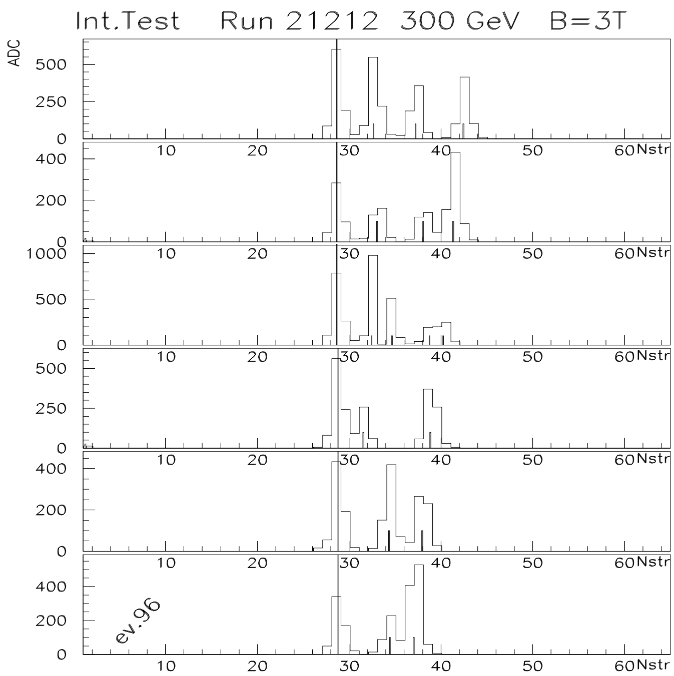


Figure 4: The example of a "good" $\mu$-track event well separated from secondaries. Muon track is selected unambiguously within the beam-profile range.

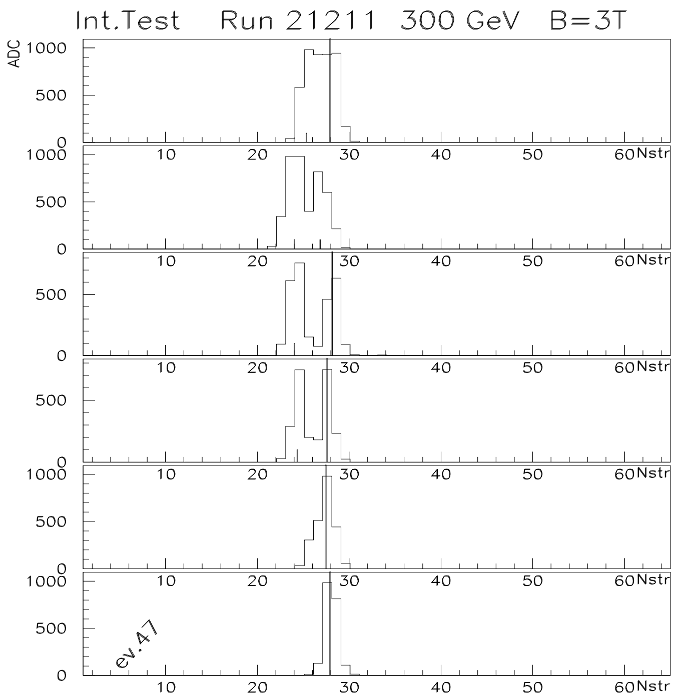


Figure 5: The example of $(\mu + e)$-track event reconstructed in a wide road. The long segments indicating the track coordinates do not lie on the same line.

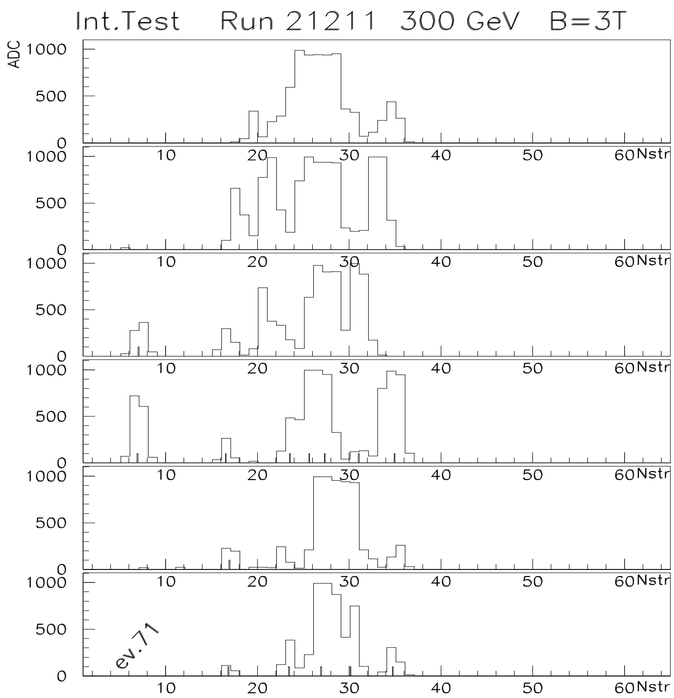


Figure 6: The example of a ”hard” event in which $\mu$-track was not reconstructed. Usually 10-20 strips are hitted in succession in every plane of the chamber with the overflow in many of them.

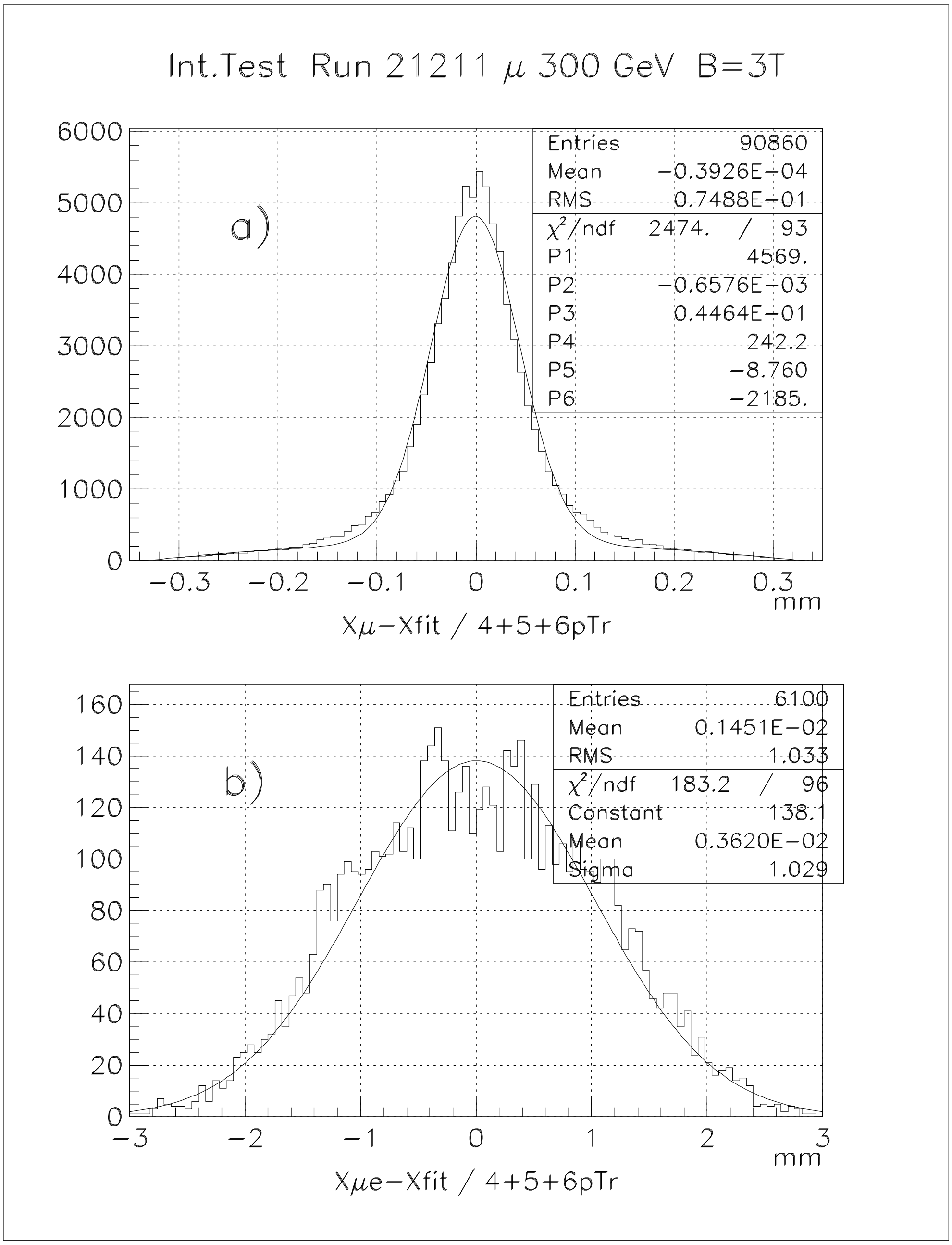


Figure 7: The residuals ($x_i - x_i^{fit}$): a) - for "good" $\mu$- tracks (histogram is fitted with Gaussian+parabola), b) - for ($\mu + e$)-tracks (fitted with Gaussian).

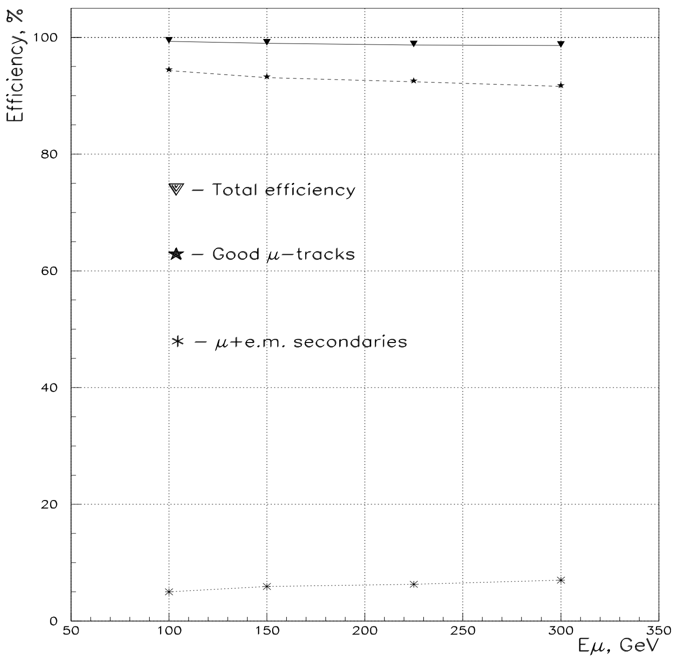


Figure 8: The efficiency of muon track reconstruction versus the energy of muon beam. The dashed line is the efficiency of ”good” $\mu$-tracks reconstruction, the dotted line - the efficiency of ($\mu$+e.m.secondaries)-tracks reconstruction and the solid line - the sum of them.

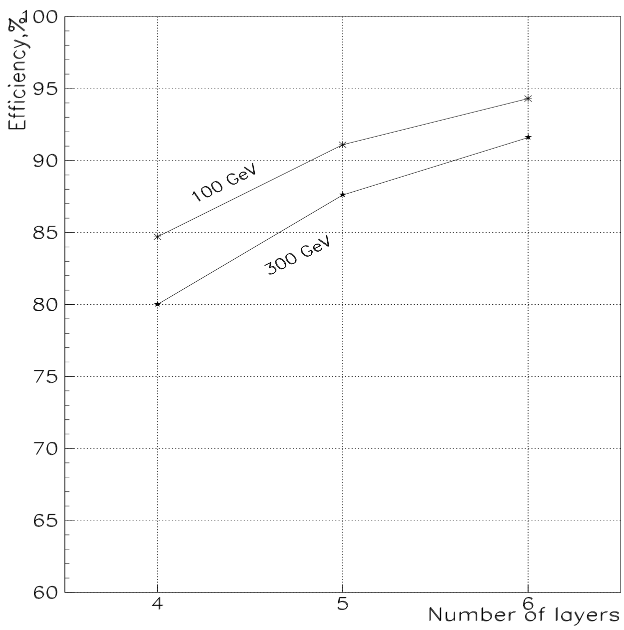


Figure 9: The muon track reconstruction efficiency dependence on the number of layers in ME1/1 chamber.

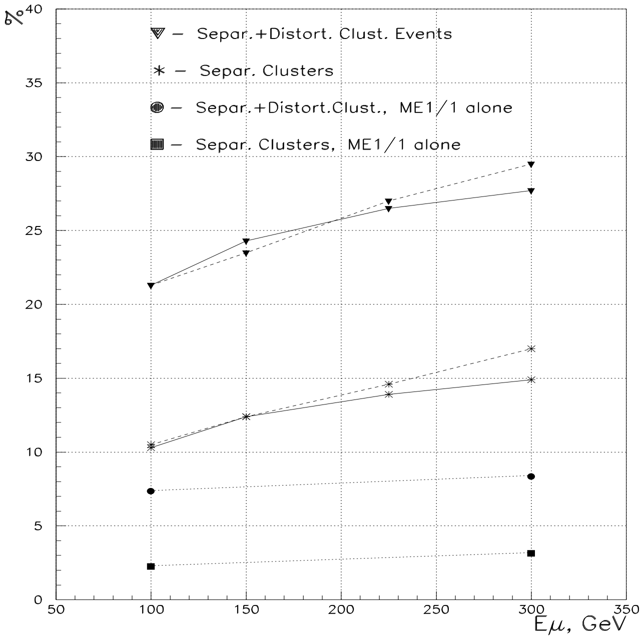


Figure 10: The fraction of events with electromagnetic secondaries versus the energy of muon beam. The solid lines are Integrated Test experimental data, the dashed line - Integrated Test GEANT-simulated data, the dotted lines - experimental data for ME1/1 stand alone without calorimeters.

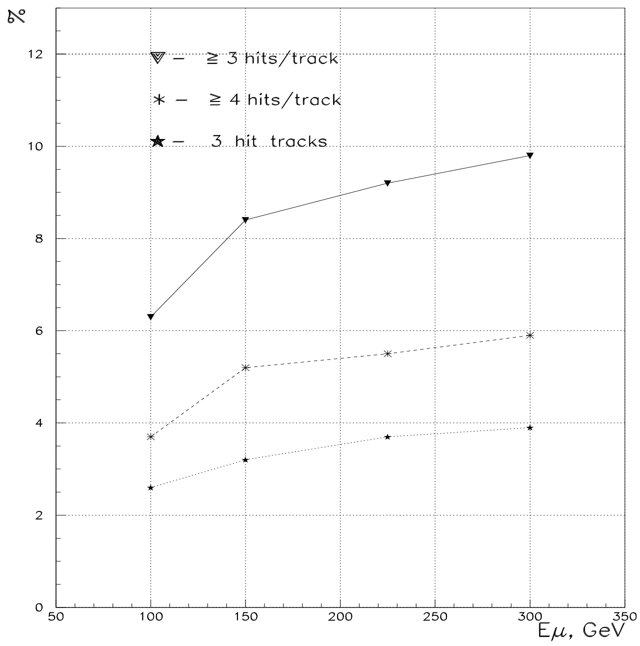


Figure 11: The fraction of events with additional to primary muon tracks versus the energy of muon beam.